February 2002

Further study of the $e^+e^- \to f\bar{f}$ process with the aid of `CalcPHEP` system

A. Andonov, D. Bardin, S. Bondarenko*,
P. Christova, L. Kalinovskaya, and G. Nanava

Laboratory for Nuclear Problems, JINR,
* *Bogoluobov Laboratory of Theoretical Physics, JINR,*
ul. Joliot-Curie 6, RU-141980 Dubna, Russia

Abstract

In this paper we complete a description of calculation of the one-loop amplitude for $e^+e^- \to f\bar{f}$ process started in CERN-TH/2001-308. This study is performed within the framework of the project `CalcPHEP`. Here we add QED subsets of the one-loop diagrams and the soft-photon contribution. The formulae we derived are realized in two independent `FORTRAN` codes, `eeffLib`, which was written in an old fashioned way, i.e. manually, and another one, created automatically with an aid of `s2n_f` (symbols to numbers) software — a part of `CalcPHEP` system. We present a comprehensive comparison between the two our codes as well as with the results existing in the world literature.

Work supported in part by INTAS N^o 00-00313.

E-mails: andonov@nusun.jinr.ru, bardin@nusun.jinr.ru, bondarenko@jinr.ru
penchris@nusun.jinr.ru, kalinov@nusun.jinr.ru, nanava@nusun.jinr.ru

Contents

List of Figures

List of Tables

Introduction

Recently, detail reports on process $e^+e^- \to t\bar{t} \to 6f$ become an active subject for energy of future electron linear colliders. This process will be one of main process and therefore must be theoretically studied profoundly (see for example the review [1]).

In this connection we consider a new calculation of $e^+e^- \to f\bar{f}$ process at the one-loop level made with an aid of computer system `CalcPHEP`, where all the calculations from the Lagrangians up to numbers are going to be eventually automatized, (see [2]).

Electroweak (EW) parts have been calculated in [3] and a very good agreement with FeynArts [4] and [5] were found.

In this paper we added lacking in [3] QED corrections. Our strategy in the descriptions of the QED part is the same as in our first paper; many definitions and notations from it are used here. References to an equation of the first part will be denoted as **(I.S.eq)** with **S** and **eq** being Section and equation numbers of Ref. [3], correspondingly.

This paper is organized in a similar fashion as [3].

In Section 1, we briefly remind the structure of one-loop amplitudes

Section 2 contains explicit expressions for all the QED *building blocks* which were not covered in [3]: QED vertices, AA and ZA boxes.

Section 3 contains the total scalar form factors of the one-loop amplitudes, now with all QED additions.

In Section 4 we present explicit expressions for helicity amplitudes made of total scalar form factors at one-loop level.

Section 5 is an Annex containing some additional expression for different QED contributions that might be derived analytically. They are not in the main stream of our paper: Lagrangian → scalar form factors → helicity amplitudes → one-loop differential cross-section. However, they are useful for pedagogical reasons, and their coding in complimentary `FORTRAN` branches of `eeffLib` provided us with powerful internal cross-checks of our codes for numerical calculations. Actually, `eeffLib` version of February'2002 has three QED branches.

Finally, Section 6 is a revised version of Section 5 of [3] in which we present again results of a comprehensive numerical comparison between `eeffLib` and `ZFITTER`. The reason for this revision is due to debugging of the December'2001 version of `eeffLib` resulting in a little change of our numbers beginning 4th or 5th digits. In this paper we also present a comparison with our another code, which was created automatically using `s2n_f` software. We also present a comprehensive comparison between the results derived with two our codes and the results existing in the world literature. In particular, we found a high precision agreement with `FeynArts` results up to 11 digits for the differential cross-sections with virtual corrections, and with resent results of [5] within 7-8 digits even with soft photons included, see [6].

1 Amplitudes

We work in the LQD basis, and the final-state fermion masses are not ignored as in previous [3]. The electron mass is ignored everywhere, but arguments of logs. Also we work in the R_ξ gauge. We checked the cancellation of ξ-dependent terms in three gauge-invariant subsets of diagrams separately. The first subset is the so-called cluster in the QED sector (or A cluster, see definitions below), the second and third are AA boxes and ZA boxes, correspondingly.

In the LQD basis, the γ and Z exchange one-loop amplitudes have the following structure:

$$A_\gamma^{\rm IBA} = i\frac{4\pi Q_e Q_f}{s}\alpha(s)\gamma_\mu \otimes \gamma_\mu\,, \tag{1.1}$$

and

$$\begin{aligned}
\mathcal{A}_Z^{\rm IBA} \;=\; & i\,e^2\frac{\chi_Z(s)}{s}\Big\{I_e^{(3)}I_t^{(3)}\gamma_\mu\gamma_+ \otimes \gamma_\mu\gamma_+ F_{LL}(s,t) + \delta_e I_t^{(3)}\gamma_\mu \otimes \gamma_\mu\gamma_+ F_{QL}(s,t) \\
& + I_e^{(3)}\delta_t\gamma_\mu\gamma_+ \otimes \gamma_\mu F_{LQ}(s,t) + \delta_e\delta_t\gamma_\mu \otimes \gamma_\mu F_{QQ}(s,t) \\
& + I_e^{(3)}I_t^{(3)}\gamma_\mu\gamma_+ \otimes (-im_t D_\mu)\, F_{LD}(s,t) + \delta_e I_t^{(3)}\gamma_\mu \otimes (-im_t D_\mu)\, F_{QD}(s,t)\Big\},
\end{aligned} \tag{1.2}$$

where *untilded* and *tilded* form factors are related by **Eqs. (I.1.11)**. Like Part I, we present all the explicit expressions in term of *untilded* quantities. Furthermore,

$$\alpha(s) = \frac{\alpha}{1 - \dfrac{\alpha}{4\pi}\Big[\Pi_{\gamma\gamma}^{\rm fer}(s) - \Pi_{\gamma\gamma}^{\rm fer}(0)\Big]} \tag{1.3}$$

is the fermionic component of the running QED coupling $\alpha(s)$ and

$$\chi_Z(s) \;=\; \frac{1}{4s_W^2c_W^2}\frac{s}{s - M_Z^2 + i\dfrac{\Gamma_Z}{M_Z}s} \tag{1.4}$$

is the Z/γ propagator ratio with an s-dependent (or constant) Z width.

2 Building Blocks (QED part)

2.1 The Zff and γff vertices

First of all we have to add vertex QED building blocks to the scalar form factors of **Eq.(I.2.60)** and finally to the complete scalar form factors of **Eqs.(I.3.117)**.

The total vertex scalar form factors $\gamma t\bar{t}$ and $Zt\bar{t}$ **Eqs. (I.2.60)** are now sums over all bosonic contributions $B = A, Z, W, H$, since we add the diagram with virtual $\gamma = A$.

All the 24 components of the total form factors in the LQD basis look like:

$$F_{L,Q,D}^{\gamma(Z)tt}(s) = F_{L,Q,D}^{\gamma(Z)A}(s) + F_{L,Q,D}^{\gamma(Z)Z}(s) + F_{L,Q,D}^{\gamma(Z)W}(s) + F_{L,Q,D}^{\gamma(Z)H}(s)\,, \tag{2.1}$$

The A cluster was formed using the same philosophy as in [3], see **Eqs. (I.2.54)-(I.2.59)**. Note, that $F_L^{\gamma A}(s)$ and $F_L^{\gamma H}(s)$ are equal to zero.

2.1.1 Library of QED Form Factors for Att clusters

Up to one-loop level, there are two diagrams, which contribute to the A cluster, see Fig. 1.

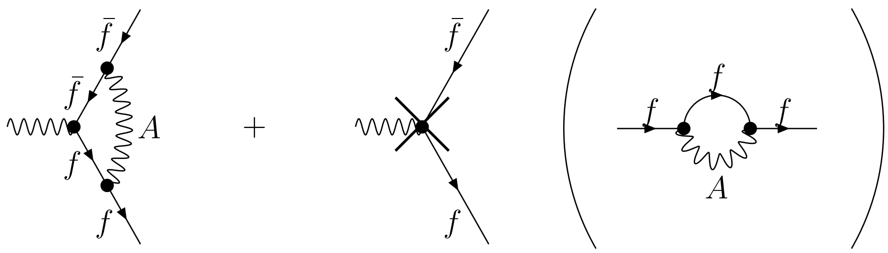

Figure 1: A cluster. One fermionic self-energy diagram in brackets gives rise to the counter term contribution depicted by the solid cross.

Since after wave function renormalization, the scalar form factors became UV-finite, instead of **Eq. (I.2.61)**, we have for all 6 form factors which are also separately gauge-invariant:

$$F_I^{\gamma(z)A} = \mathcal{F}_I^{\gamma(z)A}, \tag{2.2}$$

where $I = L, Q, D$. Individual components are:

$$\begin{aligned}
\mathcal{F}_L^{\gamma A} &= 0, \\
\mathcal{F}_Q^{\gamma A} &= Q_t^2 s_W^2 \Big\{ 2\left(s - 2m_t^2\right) C_0(-m_t^2, -m_t^2, -s; m_t, 0, m_t) \\
&\quad -3B_0^F(-s; m_t, m_t) + 3B_0^F(-m_t^2; m_t, 0) - 4m_t^2 B_{0p}(-m_t^2; 0, m_t) \Big\}, \\
\mathcal{F}_D^{\gamma A} &= -\frac{Q_t^3 s_W^2}{I_t^{(3)}} \frac{4}{\Delta_{3r}} \Big[B_0^F(-s; m_t, m_t) - B_0^F(-m_t^2; m_t, 0) \Big], \\
\mathcal{F}_L^{zA} &= \mathcal{F}_Q^{\gamma A} + Q_t^2 s_W^2 \frac{8m_t^2}{\Delta_{3r}} \Big[B_0^F(-s; m_t, m_t) - B_0^F(-m_t^2; m_t, 0) \Big], \\
\mathcal{F}_Q^{zA} &= \mathcal{F}_Q^{\gamma A} - Q_t^2 s_W^2 \frac{8m_t^2}{\Delta_{3r}} \frac{I_t^{(3)}}{\delta_t} \Big[B_0^F(-s; m_t, m_t) - B_0^F(-m_t^2; m_t, 0) \Big], \\
\mathcal{F}_D^{zA} &= -\frac{Q_t^2 s_W^2}{I_t^{(3)}} \frac{2v_t}{\Delta_{3r}} \Big[B_0^F(-s; m_t, m_t) - B_0^F(-m_t^2; m_t, 0) \Big],
\end{aligned} \tag{2.3}$$

with

$$\Delta_{3r} = 4m_t^2 - s\,. \tag{2.4}$$

2.1.2 Scalar form factor for electron case

Aee cluster is described by only one scalar form factor:

$$\begin{aligned}
\mathcal{F}^{A,e}(s) &= Q_e^2 s_W^2 \Big[2sC_0(-m_e^2, -m_e^2, -s; m_e, 0, m_e) \\
&\quad -3B_0^F(-s; m_e, m_e) + 3B_0^F(-m_e^2; m_e, 0) - 4m_e^2 B_{0p}(-m_e^2; 0, m_e) \Big].
\end{aligned} \tag{2.5}$$

2.2 Amplitudes of QED boxes

The contributions of QED AA and ZA boxes form gauge-invariant and UV finite subsets. In terms of six structures $(L,R)\otimes(L,R,D)$ they read:

$$
\begin{aligned}
\left(\mathcal{B}^{AA(ZA)}\right)^{d+c} = \; & k^{AA(ZA)}_{\rm norm}\frac{g^4}{s}\Big[\left[\gamma_\mu\gamma_+\otimes\gamma_\mu\gamma_+\right]\mathcal{F}^{AA(ZA)}_{LL}(s,t,u)+\left[\gamma_\mu\gamma_+\otimes\gamma_\mu\gamma_-\right]\mathcal{F}^{AA(ZA)}_{LR}(s,t,u)\\
+ \; & \left[\gamma_\mu\gamma_-\otimes\gamma_\mu\gamma_+\right]\mathcal{F}^{AA(ZA)}_{RL}(s,t,u)+\left[\gamma_\mu\gamma_-\otimes\gamma_\mu\gamma_-\right]\mathcal{F}^{AA(ZA)}_{RR}(s,t,u)\\
+ \; & \left[\gamma_\mu\gamma_+\otimes(-im_t ID_\mu)\right]\mathcal{F}^{AA(ZA)}_{LD}(s,t,u)+\left[\gamma_\mu\gamma_-\otimes(-im_t ID_\mu)\right]\mathcal{F}^{AA(ZA)}_{RD}(s,t,u)\Big].
\end{aligned}
\tag{2.6}
$$

where for shortening of presentation we factorize out normalization factors:

$$
k^{AA}_{\rm norm}=s^4_W Q^2_e Q^2_t\,,\qquad k^{ZA}_{\rm norm}=\frac{s^2_W Q_e Q_t}{c^2_W}\,. \tag{2.7}
$$

For completeness and subsequent use we remind $k^{ZZ}_{\rm norm}$ appearing in **Eq. (I.2.95)**:

$$
k^{ZZ}_{\rm norm}=\frac{1}{32c^4_W}\,. \tag{2.8}
$$

2.2.1 AA-box contribution

There are only two AA diagrams, *direct* and *crossed*:

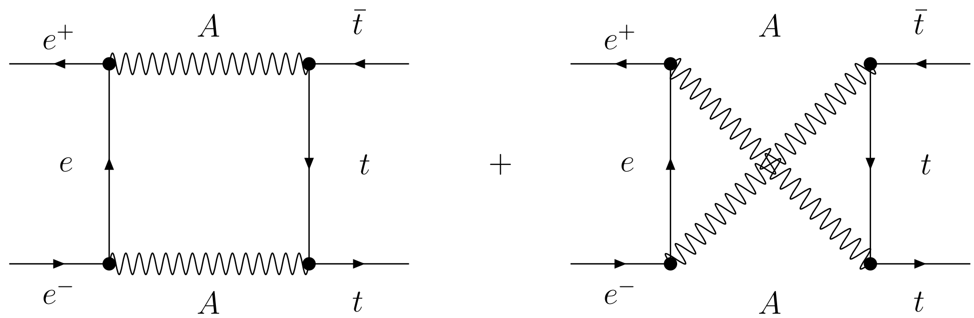

Figure 2: Direct and crossed AA boxes.

The six form factors of AA boxes might be expressed in terms of only four auxiliary functions $\mathcal{F}_1$ and $\mathcal{H}_{1,2,3}$:

$$
\begin{aligned}
\mathcal{F}^{AA}_{LL}(s,t,u) &= \mathcal{F}^{AA}_{RR}(s,t,u)=\mathcal{H}_1(s,t)-\mathcal{H}_1(s,u)+\mathcal{H}_2(s,t)+\mathcal{H}_3(s,u)\,,\\
\mathcal{F}^{AA}_{LR}(s,t,u) &= \mathcal{F}^{AA}_{RL}(s,t,u)=\mathcal{H}_1(s,t)-\mathcal{H}_1(s,u)-\mathcal{H}_2(s,u)-\mathcal{H}_3(s,t)\,,\\
\mathcal{F}^{AA}_{LD}(s,t,u) &= \mathcal{F}^{AA}_{LD}(s,t,u)=\mathcal{F}_1(s,t)-\mathcal{F}_1(s,u)\,.
\end{aligned}
\tag{2.9}
$$

The auxiliary functions are rather short:

$$
\mathcal{F}_1(s,t) = -\frac{1}{2}\frac{s}{\Delta_{4r}}\left\{\frac{1}{\Delta_{4r}}\left(-t^3_- J_{AA}(-s,-t;m_e,m_t)\right.\right.
$$

$$
\begin{aligned}
&+ts\Big[s\,C_0(-m_e^2,-m_e^2,-s;0,m_e,0)+\Big(s-2m_t^2\Big)\,C_0(-m_t^2,-m_t^2,-s;0,m_t,0)\Big]\Big)\\
&+2\frac{t}{\Delta_{3r}}\Big[2m_t^2C_0(-m_t^2,-m_t^2,-s;0,m_t,0)+B_0^F(-m_t^2;m_t,0)-B_0^F(-s;0,0)\Big]\\
&+2\frac{t}{t_-}\Big[B_0^F(-t;m_e,m_t)-B_0^F(-m_t^2;m_t,0)\Big]\Big\}, \qquad (2.10)
\end{aligned}
$$

$$
\begin{aligned}
\mathcal{H}_1\,(s,t) \;=\; & -t_-\Big[\frac{1}{2}J_{AA}(-s,-t;m_e,m_t)-C_0(-m_e^2,-m_t^2,-t;m_e,0,m_t)\Big]\\
&+\frac{s}{4\Delta_{4r}}\Big\{t_-\left(t+\frac{t_+t_-^2}{\Delta_{4r}}\right)J_{AA}(-s,-t;m_e,m_t)\\
&+2m_t^2\left(1-2\frac{t}{t_-}\right)\Big[B_0^F(-t;m_e,m_t)-B_0^F(-m_t^2;m_t,0)\Big]\Big\}, \qquad (2.11)
\end{aligned}
$$

$$
\begin{aligned}
\mathcal{H}_2\,(s,t) \;=\; & \frac{s}{4\Delta_{4r}}\Big\{\Big[-2m_t^2s+\Big(s-4m_t^2\Big)\Big(s+2t_--(st_++2tt_-)\,\frac{s}{\Delta_{4r}}\Big)\Big]\\
&\times C_0(-m_t^2,-m_t^2,-s;0,m_t,0)\\
&+(s+2t_-)\left(1-t_+\frac{s}{\Delta_{4r}}\right)s\,C_0(-m_e^2,-m_e^2,-s;0,m_e,0)\\
&-2t_-\Big[B_0^F(-t;m_e,m_t)-B_0^F(-s;0,0)\Big]\\
&-4m_t^2\Big[B_0^F(-t;m_e,m_t)-B_0^F(-m_t^2;m_t,0)\Big]\Big\}, \qquad (2.12)
\end{aligned}
$$

$$
\mathcal{H}_3\,(s,t) \;=\; \frac{s}{4\Delta_{4r}^2}\,(s+2t_-)\,t_-^3\,J_{AA}(-s,-t;m_e,m_t)\,. \qquad (2.13)
$$

Here

$$
\Delta_{4r}=-tu+m_t^4\,, \qquad (2.14)
$$

and $J^{AA}\,(Q^2,P^2;M_1,M_2)$ is due to a procedure of disentengling of the infrared divergences from D_0. Its explicit expression reads ($P^2>0, Q^2<0$, and M_1 is ignored everywhere but ln):

$$
\begin{aligned}
J^{AA}\Big(Q^2,P^2;M_1,M_2\Big)=\frac{1}{P_2+M_2^2}\Big\{&\ln\frac{(P^2+M_2^2)^2}{-Q^2P^2}\ln\left(\frac{P^2}{-Q^2}\right)-\frac{1}{2}\ln^2\left(\frac{M_1^2}{-Q^2}\right)-\frac{1}{2}\ln^2\left(\frac{M_2^2}{-Q^2}\right)\\
&+\ln^2\left(1+\frac{M_2^2}{P^2}\right)-2\mathrm{Li}_2\left(\frac{P^2}{P^2+M_2^2}\right)+i\pi\ln\left[\frac{(P^2+M_2^2)^2}{M_1^2M_2^2}\right]\Big\}. \qquad (2.15)
\end{aligned}
$$

Moreover, the relevant infrared divergent C_0 function ($P^2>0$ again), is

$$
\begin{aligned}
C_0^{\mathrm{IR}}\Big(-M_1^2,-M_2^2,P^2;M_1,\lambda,M_2\Big) \;=\; \frac{1}{2\,(P^2+M_2^2)}\Big\{&\ln\left[\frac{(P^2+M_2^2)^2}{M_1^2M_2^2}\right]\ln\frac{P^2}{\lambda^2}-2\mathrm{Li}_2\left(\frac{P^2}{P^2+M_2^2}\right)\\
&-\frac{1}{2}\ln^2\left(\frac{M_1^2}{P^2}\right)-\frac{1}{2}\ln^2\left(\frac{M_2^2}{P^2}\right)+\ln^2\left(1+\frac{M_2^2}{P^2}\right)\Big\}. \qquad (2.16)
\end{aligned}
$$

2.2.2 ZA box contribution

In R_ξ gauge there are eight ZA boxes, however, since electron mass is ignored, only four diagrams without ϕ_0 contribute:

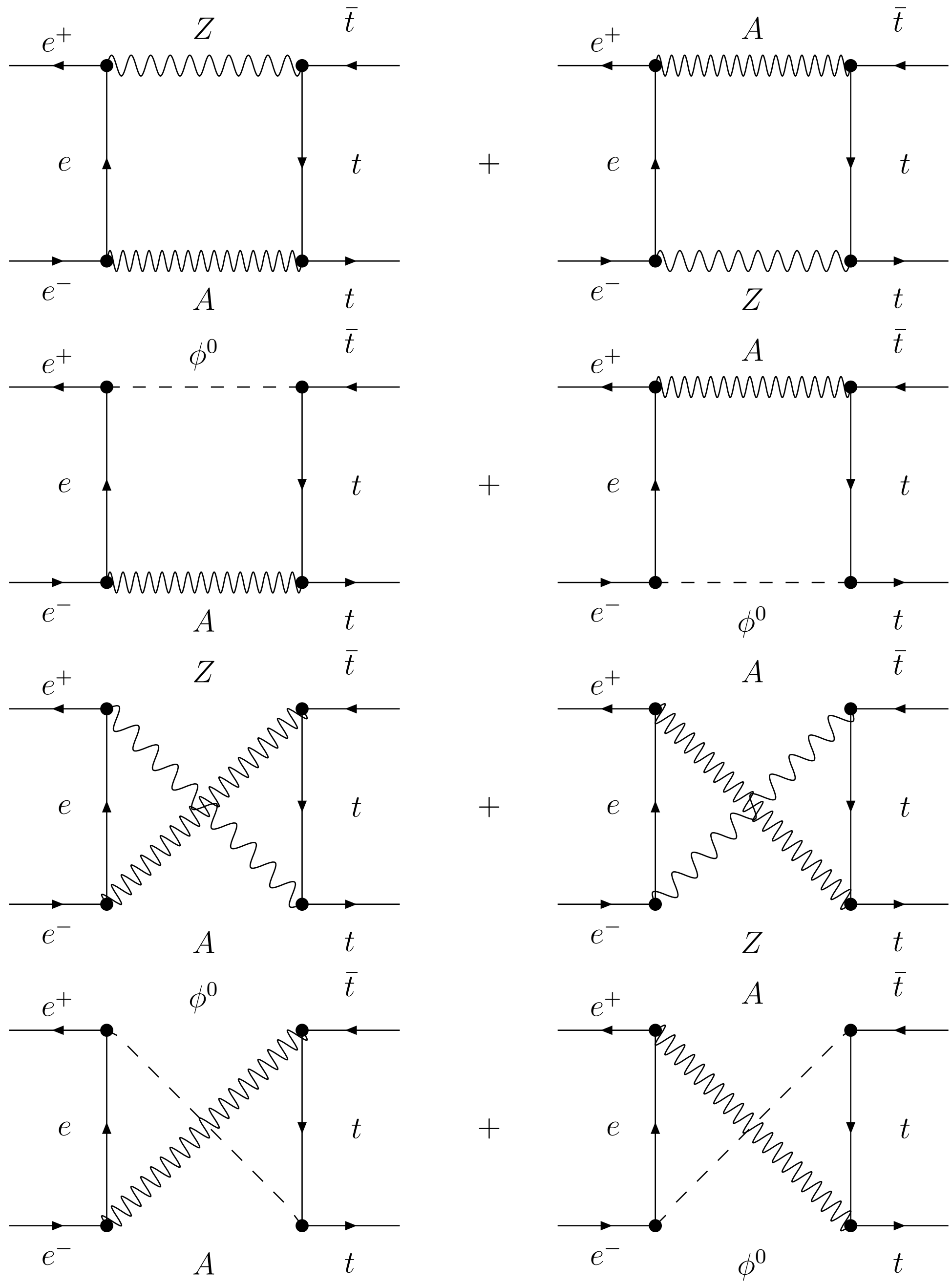

Figure 3: Direct and crossed ZA boxes.

The six relevant scalar form factors are conveniently presentable in form of differences of t and u dependent functions:

$$\mathcal{F}^{ZA}_{IJ}(s,t,u) \quad = \quad \mathcal{F}^{ZA}_{IJ}(s,t) - \mathcal{F}^{ZA}_{IJ}(s,u), \tag{2.17}$$

where index IJ is any pair of $L, R \oplus L, R, D$. The 12 $\mathcal{F}^{ZA}_{IJ}$ functions depend on 6 auxiliary functions by means of equations where the coupling constants are factored out:

$$\begin{array}{rclrcl}
\mathcal{F}^{ZA}_{LL}(s,t) &=& \sigma_e\sigma_t\mathcal{G}_1(s,t) + \sigma_e\delta_t\mathcal{G}_2(s,t)\,, & \mathcal{F}^{ZA}_{LL}(s,u) &=& \sigma_e\delta_t\mathcal{H}_1(s,u) + \sigma_e\sigma_t\mathcal{H}_2(s,u)\,,\\
\mathcal{F}^{ZA}_{RR}(s,t) &=& \delta_e\delta_t\mathcal{G}_1(s,t) + \delta_e\sigma_t\mathcal{G}_2(s,t)\,, & \mathcal{F}^{ZA}_{RR}(s,u) &=& \delta_e\sigma_t\mathcal{H}_1(s,u) + \delta_e\delta_t\mathcal{H}_2(s,u)\,,\\
\mathcal{F}^{ZA}_{LR}(s,t) &=& \sigma_e\sigma_t\mathcal{H}_1(s,t) + \sigma_e\delta_t\mathcal{H}_2(s,t)\,, & \mathcal{F}^{ZA}_{LR}(s,u) &=& \sigma_e\delta_t\mathcal{G}_1(s,u) + \sigma_e\sigma_t\mathcal{G}_2(s,u)\,,\\
\mathcal{F}^{ZA}_{RL}(s,t) &=& \delta_e\delta_t\mathcal{H}_1(s,t) + \delta_e\sigma_t\mathcal{H}_2(s,t)\,, & \mathcal{F}^{ZA}_{RL}(s,u) &=& \delta_e\sigma_t\mathcal{G}_1(s,u) + \delta_e\delta_t\mathcal{G}_2(s,u)\,,\\
\mathcal{F}^{ZA}_{LD}(s,t) &=& \sigma_e\sigma_t\mathcal{F}_1(s,t) + \sigma_e\delta_t\mathcal{F}_2(s,t)\,, & \mathcal{F}^{ZA}_{LD}(s,u) &=& \sigma_e\delta_t\mathcal{F}_1(s,u) + \sigma_e\sigma_t\mathcal{F}_2(s,u)\,,\\
\mathcal{F}^{ZA}_{RD}(s,t) &=& \delta_e\delta_t\mathcal{F}_1(s,t) + \delta_e\sigma_t\mathcal{F}_2(s,t)\,, & \mathcal{F}^{ZA}_{RD}(s,u) &=& \delta_e\sigma_t\mathcal{F}_1(s,u) + \delta_e\delta_t\mathcal{F}_2(s,u)\,.
\end{array}$$

Finally, we present these 6 auxiliary functions:

$$\begin{aligned}
\mathcal{F}_1(s,t) \;=\; & -\frac{1}{8}\frac{s}{\Delta_{4r}}\Big\{t_-\Big[\Big(R_Z+\frac{t_-}{s}-2\Big)J_{ZA}(-s,-t;m_e,m_t)\\
& -4C_0(-m_t^2,-m_e^2,-t;m_t,M_Z,m_e)\Big]\\
& +2\frac{s_-t_-}{\Delta_{4r}}\Big[tJ_{ZA}(-s,-t;m_e,m_t)+2tC_0(-m_t^2,-m_e^2,-t;m_t,M_Z,m_e)\\
& -t_-C_0(-m_e^2,-m_e^2,-s;M_Z,m_e,0)-t_+C_0(-m_t^2,-m_t^2,-s;M_Z,m_t,0)\Big]\\
& -s_+C_0(-m_e^2,-m_e^2,-s;M_Z,m_e,0)-s_-C_0(-m_t^2,-m_t^2,-s;M_Z,m_t,0)\\
& -2t\,C_0(-m_t^2,-m_e^2,-t;m_t,M_Z,m_e)-2\frac{t}{t_-}\Big[M_Z^2C_0(-m_t^2,-m_e^2,-t;m_t,M_Z,m_e)\\
& -2B_0^F(-t;m_e,m_t)+B_0^F(-m_t^2;M_Z,m_t)+B_0^F(-m_t^2;m_t,0)\Big]\\
& -2\frac{t_+}{\Delta_{3r}}\Big[\Big(M_Z^2-4m_t^2\Big)C_0(-m_t^2,-m_t^2,-s;M_Z,m_t,0)\\
& +2B_0^F(-s;M_Z,0)-B_0^F(-m_t^2;M_Z,m_t)-B_0^F(-m_t^2;m_t,0)\Big]\Big\}, \qquad (2.18)
\end{aligned}$$

$$\mathcal{F}_2(s,t) \;=\; \frac{1}{8}\frac{s}{\Delta_{4r}}\Big[\frac{t_-^2}{s}J_{ZA}(-s,-t;m_e,m_t)-2tC_0(-m_t^2,-m_e^2,-t;m_t,M_Z,m_e)\Big], \qquad (2.19)$$

$$\begin{aligned}
\mathcal{H}_1(s,t) \;=\; & -\frac{sm_t^2}{8}\Big\{\frac{1}{s}\Big[J_{ZA}(-s,-t;m_e,m_t)-2\frac{M_Z^2}{t_-}C_0(-m_t^2,-m_e^2,-t;m_t,M_Z,m_e)\Big]\\
& +\frac{1}{\Delta_{4r}}\Big(-t\Big[J_{ZA}(-s,-t;m_e,m_t)+2C_0(-m_t^2,-m_e^2,-t;m_t,M_Z,m_e)\Big]\\
& +4m_t^2C_0(-m_t^2,-m_t^2,-s;M_Z,m_t,0)+t_-\Big(R_Z-2+\frac{s_-t_+}{\Delta_{4r}}\Big)\Big[J_{ZA}(-s,-t;m_e,m_t)\\
& +2C_0(-m_t^2,-m_e^2,-t;m_t,M_Z,m_e)-2C_0(-m_t^2,-m_t^2,-s;M_Z,m_t,0)\Big]\\
& +s_-\left(s+2t_-\right)\frac{t_-}{\Delta_{4r}}\Big[C_0(-m_t^2,-m_t^2,-s;M_Z,m_t,0)
\end{aligned}$$

$$
\begin{aligned}
&-C_0(\,-m_e^2,-m_e^2,-s;M_Z,m_e,0)\Big]-s_+C_0(\,-m_e^2,-m_e^2,-s;M_Z,m_e,0)\\
&+(R_Z-1)\,(s+2t_-)\,C_0(\,-m_t^2,-m_t^2,-s;M_Z,m_t,0)\\
&-2B_0^F(\,-s;M_Z,0)+2B_0^F(\,-t;m_e,m_t)\\
&+2\frac{m_t^2}{t_-}\Big[2B_0^F(\,-t;m_e,m_t)-B_0^F(\,-m_t^2;M_Z,m_t)-B_0^F(\,-m_t^2;m_t,0)\Big]\Big)\Big\},
\end{aligned}
\tag{2.20}
$$

$$
\begin{aligned}
\mathcal{H}_2\,(s,t)\;=\;&s\Big\{-\frac{t_-}{4s_-}\Big[J_{ZA}(-s,-t;m_e,m_t)-C_0(\,-m_e^2,-m_t^2,-t;m_e,0,m_t)\\
&+C_0(\,-m_t^2,-m_e^2,-t;m_t,M_Z,m_e)\Big]+\frac{m_t^2}{8}\Big(\frac{1}{s}J_{ZA}(-s,-t;m_e,m_t)\\
&-\frac{m_t^2}{\Delta_{4r}}\Big[J_{ZA}(-s,-t;m_e,m_t)+2C_0(\,-m_t^2,-m_e^2,-t;m_t,M_Z,m_e)\Big]\Big)\Big\},
\end{aligned}
\tag{2.21}
$$

$$
\begin{aligned}
\mathcal{G}_1\,(s,t)\;=\;&s\Big\{\frac{t_-}{4s_-}\Big[-J_{ZA}(-s,-t;m_e,m_t)+C_0(\,-m_e^2,-m_t^2,-t;m_e,0,m_t)\\
&-C_0(\,-m_t^2,-m_e^2,-t;m_t,M_Z,m_e)\Big]-\frac{m_t^2}{8s}J_{ZA}(-s,-t;m_e,m_t)\\
&+\frac{1}{8\Delta_{4r}}\Big(+m_t^4\Big[J_{ZA}(-s,-t;m_e,m_t)+2C_0(\,-m_t^2,-m_e^2,-t;m_t,M_Z,m_e)\Big]\\
&-t_-\Big[-\Big(2t_+-\frac{m_t^2M_Z^2}{s}\Big)J_{ZA}(-s,-t;m_e,m_t)\\
&-4t_+C_0(\,-m_t^2,-m_e^2,-t;m_t,M_Z,m_e)+2m_t^2C_0(\,-m_t^2,-m_t^2,-s;M_Z,m_t,0)\Big]\\
&-\frac{s_-t_-t_+}{\Delta_{4r}}\Big[tJ_{ZA}(-s,-t;m_e,m_t)+2tC_0(\,-m_t^2,-m_e^2,-t;m_t,M_Z,m_e)\\
&-t_+C_0(\,-m_t^2,-m_t^2,-s;M_Z,m_t,0)-t_-C_0(\,-m_e^2,-m_e^2,-s;M_Z,m_e,0)\Big]\\
&+t\Big[s_+C_0(\,-m_e^2,-m_e^2,-s;M_Z,m_e,0)+\Big(s_+-4m_t^2\Big)\,C_0(\,-m_t^2,-m_t^2,-s;M_Z,m_t,0)\\
&+2B_0^F(\,-s;M_Z,0)-2B_0^F(\,-t;m_e,m_t)\Big]\\
&+2\frac{m_t^2t}{t_-}\Big[M_Z^2C_0(\,-m_t^2,-m_e^2,-t;m_t,M_Z,m_e)\\
&-2B_0^F(\,-t;m_e,m_t)+B_0^F(\,-m_t^2;M_Z,m_t)+B_0^F(\,-m_t^2;m_t,0)\Big]\Big)\Big\},
\end{aligned}
\tag{2.22}
$$

$$
\begin{aligned}
\mathcal{G}_2\,(s,t)\;=\;&\frac{sm_t^2}{8}\,\Big[\frac{1}{s}J_{ZA}(-s,-t;m_e,m_t)\\
&-\frac{t}{\Delta_{4r}}\Big(J_{ZA}(-s,-t;m_e,m_t)+2C_0(\,-m_t^2,-m_e^2,-t;m_t,M_Z,m_e)\Big)\Big],
\end{aligned}
\tag{2.23}
$$

where new notation were introduced for invariants

$$
s_\pm=s\pm M_Z^2\,,\qquad t_\pm=t\pm m_t^2\,,
\tag{2.24}
$$

and for the new functions $J^{IJ}\left(Q^2,P^2;M_1,M_2\right)$ (an analog of $J^{AA}\left(Q^2,P^2;M_1,M_2\right)$ Eq. (2.15)):

$$J^{AZ}\left(Q^2,P^2;M_1,M_2\right) = \frac{1}{P^2+M_2^2}\ln\left(\frac{Q^2+M_Z^2}{M_Z^2}\right)\ln\left[\frac{M_1^2M_2^2}{\left(P^2+M_2^2\right)^2}\right]. \tag{2.25}$$

2.2.3 Box–Born interferences

Any box, describing by the amplitude Eq. (2.6), interfering with γ and Z exchange tree level amplitudes, gives rise to two contributions to the differential cross-sections, which are useful for internal cross-checks:

$$\begin{aligned}\sigma_{\mathrm{BOX}\otimes\mathrm{BORN}_\gamma} \propto\ & 8Q_eQ_t\mathrm{Re}\Biggl\{\left(\left[\left(s+t_-\right)^2+sm_t^2\right]\left(\mathcal{F}_{LL}+\mathcal{F}_{RR}\right)\right.\\ & \left.+\left(sm_t^2+t_-^2\right)\left(\mathcal{F}_{LR}+\mathcal{F}_{RL}\right)-2m_t^2\left(st+t_-^2\right)\left(\mathcal{F}_{LD}+\mathcal{F}_{RD}\right)\right)\Biggr\}, \qquad (2.26)\\ \sigma_{\mathrm{BOX}\otimes\mathrm{BORN}_Z} \propto\ & 8\mathrm{Re}\Biggl\{\left(\left[\left(s+t_-\right)^2+sm_t^2\right]\delta_t\left(\sigma_e\mathcal{F}_{LL}+\delta_e\mathcal{F}_{RR}\right)\right. \qquad (2.27)\\ & +2\left(s+t_-\right)^2a_t\sigma_e\mathcal{F}_{LL}+2t_-^2a_t\delta_e\mathcal{F}_{RL}+\left(sm_t^2+t_-^2\right)\delta_t\left(\sigma_e\mathcal{F}_{LR}+\delta_e\mathcal{F}_{RL}\right)\\ & \left.+2sm_t^2a_t\left(\sigma_e\mathcal{F}_{LR}+\delta_e\mathcal{F}_{RR}\right)-2m_t^2\left(st+t_-^2\right)v_t\left(\sigma_e\mathcal{F}_{LD}+\delta_e\mathcal{F}_{RD}\right)\right)\chi_Z{}^*\Biggr\}.\end{aligned}$$

3 Total scalar form factors of the one-loop amplitude

Adding all contributions together, we observe the cancellation of all poles. The ultraviolet-finite results for six scalar form factors, replacing EW result **Eq. (I.3.118)**, are:

$$\begin{aligned}F_{LL}(s,t,u) &= \left[\mathcal{F}_L^{zee}(s)+\mathcal{F}^{A,e}(s)\right]+\mathcal{F}_L^{ztt}(s)+\mathcal{F}_{LL}^{ct}(s)+16k\mathcal{F}_{LL}^{BOX}(s,t,u),\\ F_{QL}(s,t,u) &= \left[\mathcal{F}_Q^{zee}(s)+\mathcal{F}^{A,e}(s)\right]+\mathcal{F}_L^{ztt}(s)+k\ \mathcal{F}_L^{\gamma tt}(s)+\mathcal{F}_{QL}^{ct}(s)+16k\mathcal{F}_{QL}^{BOX}(s,t,u),\\ F_{LQ}(s,t,u) &= \left[\mathcal{F}_L^{zee}(s)+\mathcal{F}^{A,e}(s)\right]+\mathcal{F}_Q^{ztt}(s)+k\ \mathcal{F}_L^{\gamma ee}(s)+\mathcal{F}_{LQ}^{ct}(s)+16k\mathcal{F}_{LQ}^{BOX}(s,t,u),\\ F_{QQ}(s,t,u) &= \left[\mathcal{F}_Q^{zee}(s)+\mathcal{F}^{A,e}(s)\right]+\mathcal{F}_Q^{ztt}(s)\\ &\quad-\frac{k}{s_W^2}\left[\mathcal{F}_Q^{\gamma ee}(s)+\mathcal{F}^{A,e}(s)+\mathcal{F}_Q^{\gamma tt}(s)\right]+\mathcal{F}_{QQ}^{ct}(s)+16k\mathcal{F}_{QQ}^{BOX}(s,t,u),\\ F_{LD}(s,t,u) &= \mathcal{F}_D^{ztt}(s)+16k\mathcal{F}_{LD}^{BOX}(s,t,u),\\ F_{QD}(s,t,u) &= \mathcal{F}_D^{ztt}(s)+k\ \mathcal{F}_D^{\gamma tt}(s)+16k\mathcal{F}_{QD}^{BOX}(s,t,u),\end{aligned} \tag{3.1}$$

where

$$k=c_W^2\left(R_Z-1\right). \tag{3.2}$$

For $IJ=LL$ component of box contribution one has:

$$\mathcal{F}_{IJ}^{BOX}(s,t,u)=k^{AA}\mathcal{F}_{IJ}^{AA}(s,t,u)+k^{ZA}\mathcal{F}_{IJ}^{ZA}(s,t,u)+k^{ZZ}\mathcal{F}_{IJ}^{ZZ}(s,t,u)+k^{WW}\mathcal{F}_{IJ}^{WW}(s,t,u) \tag{3.3}$$

and for the other components $IJ = LQ, QL, QQ, LD, QD$ of box form factors the WW box does not contribute. Moreover,

$$\mathcal{F}^{\gamma(z)tt}_{L,Q,D}(s) = \sum_{B=A,Z,H,W} \mathcal{F}^{\gamma(z)B}_{L,Q,D}(s)\ , \tag{3.4}$$

except $\mathcal{F}^{\gamma A}_{L}(s) = 0$ and $\mathcal{F}^{\gamma H}_{L}(s) = 0$.

4 Process *eett* in the helicity amplitudes

According to the analysis of the EW part in [3] and presentation of the QED part here, we have the **complete** answer for the amplitude of our process.

The aim of this section is to adapt the helicity amplitude technigues for the description of our process. We produced an alternative analityc answer for the same amplitude using the method suggested by Vega and Wudka (VW) [7].

In general, there are 16 helicity amplitude for any $2f \to 2f$ process. For the unpolarized case and when the electron mass is ignored, we are left with six independent helicity amplitudes, which depend on kinematical variables and our six form factors:

$$\begin{aligned}
\mathcal{A}_{++++} &= 0, \qquad \mathcal{A}_{+++-} = 0, \qquad \mathcal{A}_{++-+} = 0, \qquad \mathcal{A}_{++--} = 0,\\
\mathcal{A}_{+-+-} &= s\left(1-\cos\vartheta\right)\left(Q_eQ_tF_{GG} + \chi_Z\delta_e\Big[\left(1+\beta_t\right)I^{(3)}_t F_{QL} + \delta_t F_{QQ}\Big]\right),\\
\mathcal{A}_{+--+} &= s\left(1+\cos\vartheta\right)\left(Q_eQ_tF_{GG} + \chi_Z\delta_e\Big[(1-\beta_t)I^{(3)}_t F_{QL} + \delta_t F_{QQ}\Big]\right),\\
\mathcal{A}_{+---} &= \mathcal{A}_{+-++} = 2\sqrt{s}m_t\sin\vartheta\left(Q_eQ_tF_{GG} + \chi_Z\delta_e\Big[I^{(3)}_t F_{QL} + \delta_t F_{QQ} + \frac{1}{2}s{\beta_t}^2 I^{(3)}_t F_{QD}\Big]\right),\\
\mathcal{A}_{-+++} &= \mathcal{A}_{-+--} = -2\sqrt{s}m_t\sin\vartheta\Big(Q_eQ_tF_{GG}\\
&\quad +\chi_Z\Big[2I^{(3)}_e I^{(3)}_t F_{LL} + 2I^{(3)}_e\delta_t F_{LQ} + \delta_e I^{(3)}_t F_{QL} + \delta_e\delta_t F_{QQ}\\
&\quad +\frac{1}{2}s{\beta_t}^2 I^{(3)}_t\left(2I^{(3)}_e F_{LD} + \delta_e F_{QD}\right)\Big]\Big),\\
\mathcal{A}_{-++-} &= s\left(1+\cos\vartheta\right)\Big(Q_eQ_tF_{GG}\\
&\quad +\chi_Z\Big[\left(1+\beta_t\right)\left(2I^{(3)}_e I^{(3)}_t F_{LL} + \delta_e I^{(3)}_t F_{QL}\right) + \delta_t\left(2I^{(3)}_e F_{LQ} + \delta_e F_{QQ}\right)\Big]\Big),\\
\mathcal{A}_{-+-+} &= s\left(1-\cos\vartheta\right)\Big(Q_eQ_tF_{GG}\\
&\quad +\chi_Z\Big[\left(1-\beta_t\right)I^{(3)}_t\left(2I^{(3)}_e F_{LL} + \delta_e F_{QL}\right) + \delta_t\left(2I^{(3)}_e F_{LQ} + \delta_e F_{QQ}\right)\Big]\Big),\\
\mathcal{A}_{--++} &= 0, \qquad \mathcal{A}_{--+-} = 0, \qquad \mathcal{A}_{---+} = 0, \qquad \mathcal{A}_{----} = 0.
\end{aligned} \tag{4.1}$$

Here

$$\cos\vartheta = \left(t - m_t^2 + \frac{s}{2}\right)\frac{2}{s\beta_t}, \tag{4.2}$$

and for the amplitude $\mathcal{A}_{\lambda_i\lambda_j\lambda_k\lambda_l}$ each index $\lambda_{(i,j,k,l)}$ takes two values $\pm$ meaning twice projection of spins $e^+, e^-, t, \bar{t}$ onto their corresponding momentum. The differential cross-section for the unpolarized case is:

$$\frac{d\sigma}{d\cos\vartheta} = \frac{\pi\alpha^2}{s^3}\beta_t N_c \sum_{\lambda_i\lambda_j\lambda_k\lambda_l} \left|\mathcal{A}_{\lambda_i\lambda_j\lambda_k\lambda_l}\right|^2 . \tag{4.3}$$

We checked, that this expression is analytically identical to **Eq. (I.4.122)**. The expression Eq. (4.3) contains, however, spurious contributions of the two-loop order (squares of one-loop terms), which one should supress, since we would like to have a complete one-loop result.

This may be achieved with a simple trick. First of all let us note, that if all form factors are: $F_{IJ} = 1$ for $IJ = LL$, LQ, QL, QQ and $F_{IJ} = 0$ for $IJ = LD$, QD, we have the tree level. At the one-loop level LL, LQ, QL, QQ form factors may be represented as:

$$\mathbf{F}_{IJ} = 1 + \frac{\alpha}{4\pi s_W^2} F_{IJ} \,, \tag{4.4}$$

and

$$\mathbf{F}_{IJ} = \frac{\alpha}{4\pi s_W^2} F_{IJ} \,, \tag{4.5}$$

for $IJ = LD$, QD.

Instead of Eq. (4.4) for the four form factors we write

$$\mathbf{F}_{IJ} = Z + \frac{\alpha}{4\pi s_W^2} F_{IJ} \,, \tag{4.6}$$

and note that the cross section is a function of six form factors.

Then the one-loop results apparently equals:

$$\frac{d\sigma^{(1)}}{d\cos\vartheta} = \frac{d\sigma}{d\cos\vartheta}[Z=1] - \frac{d\sigma}{d\cos\vartheta}[Z=0]. \tag{4.7}$$

5 QED annex

5.1 QED vertices and soft photon contributions

Here we present virtual corrections due to QED vertices, a factorised part due to QED boxes and soft photon contributions. The expressions of this subsection can be also casted from [8].

The formal structure of factorised virtual and soft contributions is as follows:

$$\delta^{\text{virt+soft}} = \frac{\alpha}{\pi}\left[Q_e^2\delta_{\text{ISR}}^{\text{virt+soft}} + Q_e Q_t \delta_{\text{IFI}}^{\text{virt+soft}} + Q_t^2\delta_{\text{FSR}}^{\text{virt+soft}}\right]. \tag{5.1}$$

There are three types of contributions: ISR, FSR and IFI.

5.1.1 Initial state radiation (ISR)

Contributions of the initial state QED $e^+e^-\gamma$ vertex and ISR soft are short, since electron mass is ignored:

$$\begin{aligned}
\delta^{\rm virt}_{\rm ISR} &= -\ln\frac{m_e^2}{\lambda^2}\Bigl(l_e-1\Bigr)-\frac{1}{2}l_e^2+\frac{3}{2}l_e-2+4{\rm Li}_2\left(1\right), \\
\delta^{\rm soft}_{\rm ISR} &= \ln\left(\frac{4\omega^2}{s}\frac{m_e^2}{\lambda^2}\right)\Bigl(l_e-1\Bigr)+\frac{1}{2}l_e^2-2{\rm Li}_2\left(1\right),
\end{aligned} \tag{5.2}$$

where

$$l_e=\ln\left(\frac{s}{m_e^2}\right). \tag{5.3}$$

5.1.2 Initial–final state interference (IFI)

This originates from contributions of QED boxes: $\gamma\gamma, Z\gamma$ and initial–final state soft photons interference:

$$\delta^{\rm virt}_{\rm IFI} = -2\ln\frac{s}{\lambda^2}\ln\frac{t_-}{u_-}, \tag{5.4}$$

$$\delta^{\rm soft}_{\rm IFI} = 2\ln\frac{4\omega^2}{\lambda^2}\ln\frac{t_-}{u_-}+\Bigl[F^{\rm soft}\left(s,t\right)-F^{\rm soft}\left(s,u\right)\Bigr], \tag{5.5}$$

with

$$\begin{aligned}
F^{\rm soft}\left(s,t\right) &= -\frac{1}{2}l_e^2-\frac{1}{2}\ln^2\eta+2\ln\eta\ln\left(1+\frac{2m_t^2}{\beta_+t_-}\right) \\
&\quad -\ln^2\left(1+\frac{2m_t^2}{\beta_+t_-}\right)+\ln^2\left(-\frac{st}{t_-^2}\right)+2\ln\left(-\frac{st}{t_-^2}\right)\ln\left(1+\frac{t_-^2}{st}\right) \\
&\quad +2{\rm Li}_2\left(1-\frac{2t}{t_-\beta_+}\right)-2{\rm Li}_2\left(\frac{-\beta_-t_-}{\beta_+t_-+2m_t^2}\right)-2{\rm Li}_2\left(-\frac{t_-^2}{st}\right)-2{\rm Li}_2\left(1\right),
\end{aligned} \tag{5.6}$$

where we introduce the notations

$$\beta\equiv\beta_t=\sqrt{1-\frac{4m_t^2}{s}}\,,\qquad \beta_+=1+\beta\,,\qquad \beta_-=1-\beta\,,\qquad \eta=\frac{\beta_-}{\beta_+}\,. \tag{5.7}$$

5.1.3 Final state radiation (FSR)

Contributions of one-loop QED $f\bar{f}\gamma$ vertex and final state soft photon radiation are:

$$\begin{aligned}
\delta^{\rm virt}_{\rm FSR} &= -\ln\frac{m_t^2}{\lambda^2}\Bigl[-\frac{(1+\beta^2)}{2\beta}\ln\eta-1\Bigr]-\frac{3}{2}\beta\ln\eta-2 \\
&\quad +\frac{(1+\beta^2)}{2\beta}\Bigl[-\frac{1}{2}\ln^2\eta+2\ln\eta\ln\left(1-\eta\right)+2{\rm Li}_2\left(\eta\right)+4{\rm Li}_2\left(1\right)\Bigr],
\end{aligned}$$

$$\delta^{\rm soft}_{\rm FSR} = \ln\frac{4\omega^2}{\lambda^2}\Bigl[-\frac{(1+\beta^2)}{2\beta}\ln\eta-1\Bigr]-\frac{1}{\beta}\ln\eta$$
$$+\frac{(1+\beta^2)}{2\beta}\Bigl[-\frac{1}{2}\ln^2\eta+2\ln\eta\ln(1-\eta)+2{\rm Li}_2(\eta)-2{\rm Li}_2(1)\Bigr]. \tag{5.8}$$

Contribution of the ISR Eq. (5.2) may be received from these expressions in the limit $m_t = m_e \to 0$.

5.1.4 Non-factorized final state vertex 'anomalous' contributions

For presentation of this contribution let us introduce the definition

$$L_n = \ln\frac{\beta-1}{\beta+1}. \tag{5.9}$$

The 'anomalous' part of QED vertex contribution to the differential cross-section reads:

$$\frac{d\sigma^a}{d\cos\vartheta} = 4\alpha^3 N_c\frac{m_t^2}{s^4}Q_t^2\Biggl[\Bigl(Q_e^2Q_t^2+2Q_eQ_tv_ev_tRe(\chi_Z)+\left(v_e^2+a_e^2\right)v_t^2|\chi_Z|^2\Bigr)\left(st+t_-^2\right)Re(L_n)$$
$$+Q_eQ_ta_ea_ts\,(s+2t_-)\,Re(L_n\chi_Z)$$
$$+\Biggl(\left(v_e^2+a_e^2\right)a_t^2\left[s\left(s-4m_t^2\right)+2\left(st+t_-^2\right)\right]$$
$$+2v_ea_ev_ta_ts\,(s+2t_-)\Biggr)|\chi_Z|^2Re(L_n)\Biggr]. \tag{5.10}$$

5.2 An alternative form of the cross-section for QED boxes

Here we present some useful formulae which are not in the main stream of our approach (described in previous Sections), but that were used for internal cross checks of calculations of the QED part of the process under consideration.

The QED boxes Eqs. (2.26) and (2.27) may be greatly simplified purely algebraically. For the sum of AA and ZA boxes one may easily derive the cross-section:

$$\frac{d\sigma^{\rm BOX}}{d\cos\vartheta} = \frac{2\alpha^3}{s}\beta Q_eQ_tN_c\,{\rm Re}\Bigl\{Q_e^2Q_t^2\,\mathcal{F}_V+Q_eQ_t\,\chi_Z\Bigl[v_ev_t\left(\mathcal{F}_V^*+\mathcal{H}_V\right)+a_ea_t\left(\mathcal{F}_A^*+\mathcal{G}_V\right)\Bigr]$$
$$+|\chi_Z|^2\Bigl[\left(v_e^2+a_e^2\right)\left(v_t^2\mathcal{H}_V+a_t^2\mathcal{H}_A\right)+2a_ev_ea_tv_t\,\left(\mathcal{G}_V+\mathcal{G}_A\right)\Bigr]\Bigr\}, \tag{5.11}$$

where $\chi_Z(s)$ is defined by Eq. (1.4) and the six *cross-section form fartors* are:

$$\begin{aligned}
\mathcal{F}_V &= \mathcal{F}_V(t)-\mathcal{F}_V(u),\\
\mathcal{F}_A &= \mathcal{F}_A(t)+\mathcal{F}_A(u),\\
\mathcal{H}_V &= \mathcal{H}_V(t)-\mathcal{H}_V(u),\\
\mathcal{H}_A &= \mathcal{H}_A(t)-\mathcal{H}_A(u),\\
\mathcal{G}_V &= \mathcal{G}_V(t)+\mathcal{G}_V(u),\\
\mathcal{G}_A &= \mathcal{G}_A(t)+\mathcal{G}_A(u),
\end{aligned} \tag{5.12}$$

with

$$
\begin{aligned}
\mathcal{F}_{V}(t) &= \frac{1}{s}\Big\{\frac{t_-}{4}\Big[2m_t^2+(s+2t_-)\Big]J_{AA}(-s,-t;m_e,m_t)\\
&+t\Big(\frac{1}{2}\Big[sC_0(-m_e^2,-m_e^2,-s;0,m_e,0)+\Big(s-4m_t^2\Big)C_0(-m_t^2,-m_t^2,-s;0,m_t,0)\Big]\\
&+\frac{2m_t^2}{\Delta_{3r}}\Big[2m_t^2C_0(-m_t^2,-m_t^2,-s;0,m_t,0)+B_0^F(-m_t^2;m_t,0)-B_0^F(-s;0,0)\Big]\Big)\\
&-\frac{sm_t^2}{t_-}\Big[B_0^F(-t;m_e,m_t)-B_0^F(-m_t^2;m_t,0)\Big]\\
&-\frac{(s+t_-)}{2}\Big[B_0^F(-t;m_e,m_t)-B_0^F(-s;0,0)\Big]\Big\}, \qquad (5.13)
\end{aligned}
$$

$$
\begin{aligned}
\mathcal{F}_{A}(t) &= \frac{1}{s}\Big\{\frac{s+2t_-}{4}t_-J_{AA}(-s,-t;m_e,m_t)-m_t^2\Big(\frac{1}{2}sC_0(-m_t^2,-m_t^2,-s;0,m_t,0)\\
&+\left(\frac{s}{t_-}+1\right)\Big[B_0^F(-t;m_e,m_t)-B_0^F(-m_t^2;m_t,0)\Big]\Big)\\
&-\frac{(s+t_-)}{2}\Big[B_0^F(-t;m_e,m_t)-B_0^F(-s;0,0)\Big]\Big\}, \qquad (5.14)
\end{aligned}
$$

$$
\begin{aligned}
\mathcal{H}_0(t) &= \frac{1}{s^2}\Big\{-\Big(t_-^2+(s+t_-)^2\Big)t_-\Big[J_{ZA}(-s,-t;m_e,m_t)-\frac{1}{2}J_{AA}(-s,-t;m_e,m_t)\\
&+C_0(-m_t^2,-m_e^2,-t;m_t,M_Z,m_e)\Big]\\
&+s_-\Big(t_-\,(s_++2t)\Big[\frac{1}{2}J_{ZA}(-s,-t;m_e,m_t)+C_0(-m_t^2,-m_e^2,-t;m_t,M_Z,m_e)\Big]\\
&+\frac{sm_t^2}{t_-}\Big[M_Z^2C_0(-m_t^2,-m_e^2,-t;m_t,M_Z,m_e)-2B_0^F(-t;m_e,m_t)\\
&+B_0^F(-m_t^2;m_t,0)+B_0^F(-m_t^2;M_Z,m_t)\Big]\\
&+st\Big[C_0(-m_e^2,-m_e^2,-s;M_Z,m_e,0)+C_0(-m_t^2,-m_t^2,-s;M_Z,m_t,0)\Big]\\
&-(s+t_-)\Big[B_0^F(-t;m_e,m_t)-B_0^F(-s;M_Z,0)\Big]\Big)\Big\}, \qquad (5.15)
\end{aligned}
$$

$$
\begin{aligned}
\mathcal{H}_{V}(t) &= \mathcal{H}_0(t)+\frac{2m_t^2}{s^2}\Big\{-st_-\Big[J_{ZA}(-s,-t;m_e,m_t)-\frac{1}{2}J_{AA}(-s,-t;m_e,m_t)\\
&+C_0(-m_t^2,-m_e^2,-t;m_t,M_Z,m_e)\Big]\\
&+s_-t\Big(-C_0(-m_t^2,-m_t^2,-s;M_Z,m_t,0)+\frac{1}{\Delta_{3r}}\Big[s_-C_0(-m_t^2,-m_t^2,-s;M_Z,m_t,0)\\
&+B_0^F(-m_t^2;m_t,0)+B_0^F(-m_t^2;M_Z,m_t)-2B_0^F(-s;M_Z,0)\Big]\Big)\Big\}, \qquad (5.16)
\end{aligned}
$$

$$
\mathcal{H}_{A}(t) = \mathcal{H}_0(t)+\frac{2m_t^2}{s^2}\Big\{t_-\Big[M_Z^2J_{ZA}(-s,-t;m_e,m_t)
$$

$$
\begin{aligned}
& -s\left(\frac{1}{2}J_{AA}(-s,-t;m_e,m_t)-C_0(-m_t^2,-m_e^2,-t;m_t,M_Z,m_e)\right)\Big]\\
& +s_-\Big[-tC_0(-m_t^2,-m_t^2,-s;M_Z,m_t,0)+s_+C_0(-m_t^2,-m_e^2,-t;m_t,M_Z,m_e)\\
& -B_0^F(-t;m_e,m_t)+B_0^F(-s;M_Z,0)\Big]\Big\}, \qquad (5.17)
\end{aligned}
$$

$$
\begin{aligned}
\mathcal{G}_V(t) \;=\; & -\frac{1}{s}\Big\{(s+2t_-)\,t_-\Big[J_{ZA}(-s,-t;m_e,m_t)\\
& -\frac{1}{2}J_{AA}(-s,-t;m_e,m_t)+C_0(-m_t^2,-m_e^2,-t;m_t,M_Z,m_e)\Big]\\
& -s_-\Big(\frac{t_-}{s}(s_++2t_-)\left[\frac{1}{2}J_{ZA}(-s,-t;m_e,m_t)+C_0(-m_t^2,-m_e^2,-t;m_t,M_Z,m_e)\right]\\
& +\frac{1}{2}M_Z^2\Big[C_0(-m_e^2,-m_e^2,-s;M_Z,m_e,0)+C_0(-m_t^2,-m_t^2,-s;M_Z,m_t,0)\Big]\\
& +m_t^2\Big(2C_0(-m_t^2,-m_e^2,-t;m_t,M_Z,m_e)+\frac{1}{t_-}\Big[M_Z^2C_0(-m_t^2,-m_e^2,-t;m_t,M_Z,m_e)\\
& -2B_0^F(-t;m_e,m_t)+B_0^F(-m_t^2;m_t,0)+B_0^F(-m_t^2;M_Z,m_t)\Big]\\
& -\frac{(s+t_-)}{s}\Big[B_0^F(-t;m_e,m_t)-B_0^F(-s;M_Z,0)\Big]\Big)\Big\}, \qquad (5.18)
\end{aligned}
$$

$$
\begin{aligned}
\mathcal{G}_A(t) \;=\; & \mathcal{G}_V(t)-m_t^2\frac{s_-}{s^2}\Big[2s_-C_0(-m_t^2,-m_e^2,-t;m_t,M_Z,m_e)\\
& +s_+C_0(-m_t^2,-m_t^2,-s;M_Z,m_t,0)\\
& +2B_0^F(-t;m_e,m_t)-B_0^F(-m_t^2;M_Z,m_t)-B_0^F(-m_t^2;m_t,0)\Big]. \qquad (5.19)
\end{aligned}
$$

The Eqs. (5.11)–(5.19) were coded as a separate branch of `eettLib` and together with vertex QED contributions described in the previous subsections was used for internal cross-check of QED part of calculations.

Some factorized part of the AA and ZA boxes contribution is not included in Eq. (5.11). It has a form

$$
\frac{d\sigma}{d\cos\vartheta}\frac{\alpha}{\pi}Q_eQ_t\delta^{\rm virt}_{\rm IFI}, \qquad (5.20)
$$

where $\delta^{\rm virt}_{\rm IFI}$ is given by Eq. (5.4).

The whole QED contribution can be written as follows

$$
\frac{d\sigma^{\rm QED}}{d\cos\vartheta}=\frac{d\sigma^{\rm BORN}}{d\cos\vartheta}\delta^{\rm virt+soft}+\frac{d\sigma^{a}}{d\cos\vartheta}+\frac{d\sigma^{\rm BOX}}{d\cos\vartheta}, \qquad (5.21)
$$

where $\delta^{\rm virt+soft}$ is defined by Eqs. (5.1)–(5.8).

6 Numerical results and discussion

All the formulae derived in this paper as well as in Ref. [3] are realized in a FORTRAN code with a tentative name eeffLib. Numbers presented in this section are produced with updated, February 2002, version of the code. As compared to December 2000 version, used to produce numbers for Ref. [3], current version contains full QED corrections together with the soft photon contribution to the angular distribution $d\sigma/d\cos\vartheta$. Morever, two bugs of December 2000 version were fixed, which resulted in a change of numbers. First, for light final state fermion masses, the numerical precision was being lost. After curing this oddity, the agreement between eeffLib and ZFITTER numbers became even better. Secondly, there was a bug in a part of FORTRAN code computing ZZ box contribution. Its fixing resulted in a change of numbers (in 4th–5th digits) for the case of heavy final state fermion masses (top quark). Since numbers which were presented in Ref. [3] are changed anyway, we decided to present again all the Tables that were already given in Ref. [3]. On top of it, we will show several new examples of numbers. In particular, we will show a comparison of the electroweak form factors (EWFF) *including* QED corrections between eeffLib and another FORTRAN code, which was automatically generated from form log files with the aid of a system s2n_f (*symbolic to numbers*), producing a FORTRAN source code — a part of our CalcPHEP system. This comparison provides a powerful internal cross-check of our numerics that practically excludes appearance of bugs of a kind discussed above.

We begin with showing several examples of comparison with ZFITTER v6.30 [9]. In the present realization, eeffLib does not calculate M_W from μ decay and does not precompute either Sirlin's parameter Δr or total Z width, which enters the Z boson propagator. For this reason, the three parameters: M_W , Δr , Γ_Z were being taken from ZFITTER and used as INPUT for eeffLib. Moreover, present eeffLib is a purely one-loop code, while in ZFITTER it was not foreseen to access just one-loop form factors with users flags. To accomplish the goals of comparison at the one-loop level, we had to modify the DIZET electroweak library. The most important change was an addition to the SUBROUTINE ROKANC:

```
*
* For eett
*
      FLL=(XROK(1)-1D0+DR )*R1/AL4PI
      FQL=FLL+(XROK(2)-1D0)*R1/AL4PI
      FLQ=FLL+(XROK(3)-1D0)*R1/AL4PI
      FQQ=FLL+(XROK(4)-1D0)*R1/AL4PI
```

with the aid of which we reconstruct four form factors from ZFITTER's effective couplings ρ and κ's (F_{LD} and F_{QD} do not contribute in massless approximation).

6.1 Flags of eeffLib

Here we give a description of flags (user options) of eeffLib. While creating the code, we followed the principle to preserve as much as possible the meaning of flags as described in the ZFITTER description [10]. In the list below, a comment 'as in ZFD' means that the flag has exactly the same meaning as in [10]. Here we describe an extended set of flags of February 2002 version of `eeffLib`.

- `ALEM=3  ! as in ZFD`
- `ALE2=3  ! as in ZFD`
- `VPOL=0  ! =0` $\alpha(0)$; =1,=2 as in ZFD; =3 is reserved for later use
  Note that the flag is extended to `VPOL=0` to allow calculations 'without running of α'.
- `QCDC=0  ! as in ZFD`
- `ITOP=1  ! as in DIZET (internal flag)`
- `GAMS=1  ! as in ZFD`
- `WEAK=1  ! as in ZFD` (use `WEAK=2` in v6.30 to throw away some higher order terms)
- `IMOMS=1 ! =0` α-scheme; =1 GFermi-scheme
  New meaning of an old flag: switches between two renormalization schemes;
- `BOXD=6`
  Together with `WEAK=0` is used for an internal comparison of separate boxes and QED contributions:
  `BOXD ! =1` with $\gamma\gamma$ boxes
  `! =2` with $Z\gamma$ boxes
  `! =3` with $\gamma\gamma$ and $Z\gamma$ boxes
  `! =4` with all QED contributions
  Together with `WEAK=1` (working option), it has somewhat different meaning:
  `BOXD ! =0` without any boxes
  `! =1` with $\gamma\gamma$ boxes
  `! =2` with $Z\gamma$ boxes
  `! =3` with $\gamma\gamma$ and $Z\gamma$ boxes
  `! =4` with WW boxes
  `! =5` with WW and ZZ boxes
  `! =6` with all QED and EW boxes

'Treatment' options.

- `GAMZTR=1` treatment of Γ_Z.
  The option is implemented for the sake of comparison with `FeynArts`:
  `GAMZTR=0` $\Gamma_Z = 0$
  `GAMZTR=1` $\Gamma_Z \neq 0$
- `EWFFTR=0` treatment of EW form factors.
  Switches between form factors and effective `ZFITTER` couplings ρ and κ's. The option is implemented for comparison with `ZFITTER`:
  `EWFFTR=0` electroweak form factors
  `EWFFTR=1` effective coullings ρ and κ
- `FERMTR=1` treatment of fermionic masses.
  Switches between three different sets of 'effective quark masses':
  `FERMTR=1` a 'standard' set of fermions masses
  `FERMTR=2,3` 'modified' sets

- `VPOLTR=1` treatment of photonic vacuum polarization.
  Switches between lowest order expression, $\alpha(s) = \alpha\left[1+\Delta\alpha(s)\right]$, and its 'resummed' version, $\alpha(s) = \alpha/\left[1-\Delta\alpha(s)\right]$:
  `VPOLTR=0` lowest order
  `VPOLTR=1` resummed
- `EWRCTR=2` treatment of electroweak radiative corrections.
  Switches between three variants for vertex corrections:
  `EWRCTR=0` electroweak form factors contain only QED additions
  `EWRCTR=1` electroweak form factors do not contain QED additions
  `EWRCTR=2` electroweak form factors contain both QED and EW additions
- `EMASTR=0` treatment of terms with $\ln(s/m_e^2)$ in $\gamma\gamma$ and $Z\gamma$ boxes, which are present in various functions but cancel in sum:
  `EMASTR=0` these terms are suppressed in all functions which they enter
  `EMASTR=1` these terms are retained in all functions which results in loosing of computer precision owing to numerical cancellation; results for `EMASTR=0` and `EMASTR=1` are equal
- `EWWFFV=1` treatment of vertex and box diagrams with virtual W boson, switches between two variants:
  `EWWFFV=0` variant of formulae without b-quark mass
  `EWWFFV=1` variant of formulae with finite b-quark mass

Options affecting QED contributions.

- `IQED=4` variants of inclusion virtual and soft photon QED contributions:
  `IQED=1` only initial state radiation (ISR)
  `IQED=2` only initial–final interference (IFI)
  `IQED=3` only final state radiation (FSR)
  `IQED=4` all QED contributions are included
- `IBOX=4` is active only if `IQED`=2 or 4 and affects only Eq. (5.11):
  `IBOX=0` AA boxes interfering with γ exchange BORN
  `IBOX=1` AA boxes
  `IBOX=2` ZA boxes
  `IBOX=3 or 4` AA+ZA boxes

6.2 `eeffLib`–`ZFITTER` comparison of scalar form factors

First of all we discuss the results of a computation of the four scalar form factors,

$$F_{LL}(s,t)\,,\quad F_{QL}(s,t)\,,\quad F_{LQ}(s,t)\,,\quad F_{QQ}(s,t)\,, \tag{6.1}$$

for three variants:
1) without EW boxes, i.e. without gauge-invariant contribution of ZZ boxes, and without $\xi=1$ part of the WW box, Eq. **(I.2.93)**;
2) with WW boxes;
3) with WW and ZZ boxes.

Table 1: EWFF for the process $e^+e^- \to u\bar{u}$. `eeffLib`–`ZFITTER` comparison.

Without EW boxes				
$\sqrt{s}$		100 GeV	200 GeV	300 GeV
FF	μ			
F_{LL}	$M_W/10$	$13.47773 - i1.84784$	$16.22034 - i10.49412$	$23.75240 - i11.27469$
	M_W	$13.47773 - i1.84784$	$16.22034 - i10.49412$	$23.75240 - i11.27469$
	$10M_W$	$13.47773 - i1.84784$	$16.22034 - i10.49412$	$23.75240 - i11.27469$
`ZFITTER`		$13.47771 - i1.84786$	$16.22031 - i10.49405$	$23.75237 - i11.27464$
F_{QL}	$M_W/10$	$29.34721 + i3.67330$	$30.33891 + i3.34531$	$31.64553 + i2.75258$
	M_W	$29.34721 + i3.67330$	$30.33891 + i3.34531$	$31.64553 + i2.75258$
	$10M_W$	$29.34721 + i3.67330$	$30.33891 + i3.34531$	$31.64553 + i2.75258$
`ZFITTER`		$29.34720 + i3.67330$	$30.33889 + i3.34535$	$31.64552 + i2.75259$
F_{LQ}	$M_W/10$	$29.13302 + i3.26972$	$30.03854 + i1.54158$	$31.68636 - i0.22635$
	M_W	$29.13302 + i3.26972$	$30.03854 + i1.54158$	$31.68636 - i0.22635$
	$10M_W$	$29.13302 + i3.26972$	$30.03854 + i1.54158$	$31.68636 - i0.22635$
`ZFITTER`		$29.13304 + i3.26973$	$30.03855 + i1.54163$	$31.68635 - i0.22634$
F_{QQ}	$M_W/10$	$44.90390 + i8.85688$	$43.80286 + i10.02412$	$44.21223 + i10.83899$
	M_W	$44.90390 + i8.85688$	$43.80286 + i10.02412$	$44.21223 + i10.83899$
	$10M_W$	$44.90390 + i8.85688$	$43.80286 + i10.02412$	$44.21223 + i10.83899$
`ZFITTER`		$44.90392 + i8.85688$	$43.80285 + i10.02411$	$44.21224 + i10.83894$
WW is added				
F_{LL}	$M_W/10$	$12.94469 - i1.84784$	$9.34066 - i9.42482$	$9.03908 - i11.55971$
	M_W	$12.94469 - i1.84784$	$9.34066 - i9.42482$	$9.03908 - i11.55971$
	$10M_W$	$12.94469 - i1.84784$	$9.34066 - i9.42482$	$9.03908 - i11.55971$
`ZFITTER`		$12.94468 - i1.84786$	$9.34065 - i9.42467$	$9.03903 - i11.55958$

In this comparison we use flags as in subsection 6.1 and, moreover,

$$
\begin{aligned}
M_W &= 80.4514958 \text{ GeV}, \\
\Delta r &= 0.0284190602\,, \\
\Gamma_Z &= 2.499776 \text{ GeV}.
\end{aligned}
\qquad (6.2)
$$

In Table 1 we show an example of comparison of four form factors $F_{LL,QL,LQ,QQ}(s,t)$ between the `eeffLib`, where we set $m_t = 0.2$ GeV and `ZFITTER` (the latter is able to deliver only massless results). The form factors are shown as complex numbers for the three c.m.s. energies (for $t = m_t^2 - s/2$) and for the three values of scale $\mu = M_W/10,\ M_W,\ 10M_W$. The table demonstrates scale independence and very good agreement with `ZFITTER` results (6 or 7 digits). One should stress that total agreement with `ZFITTER` is not expected because in the `eeffLib` code we use massive expressions to compute the nearly massless case. Certain numerical cancellations leading to losing some numerical precision are expected. We should conclude that the agreement is very good and uniquely demonstrates that our formulae have the correct $m_t \to 0$ limit.

Table 2: EWFF for the process $e^+e^- \to u\bar{u}$. eeffLib–ZFITTER comparison.

With ZZ boxes				
$\sqrt{s}$		100 GeV	200 GeV	300 GeV
FF	μ			
F_{LL}	$M_W/10$	$12.89584 - i1.84784$	$8.24736 - i10.64666$	$8.98375 - i12.88478$
	M_W	$12.89584 - i1.84784$	$8.24736 - i10.64666$	$8.98375 - i12.88478$
	$10M_W$	$12.89584 - i1.84784$	$8.24736 - i10.64666$	$8.98375 - i12.88478$
ZFITTER		$12.89583 - i1.84786$	$8.24736 - i10.64651$	$8.98370 - i12.88466$
F_{QL}	$M_W/10$	$29.30447 + i3.67330$	$29.38219 + i2.27610$	$31.59711 + i1.59302$
	M_W	$29.30447 + i3.67330$	$29.38219 + i2.27610$	$31.59711 + i1.59302$
	$10M_W$	$29.30447 + i3.67330$	$29.38219 + i2.27610$	$31.59711 + i1.59302$
ZFITTER		$29.30445 + i3.67330$	$29.38216 + i2.27613$	$31.59710 + i1.59304$
F_{LQ}	$M_W/10$	$29.10829 + i3.26972$	$29.48510 + i0.92307$	$31.65836 - i0.89713$
	M_W	$29.10829 + i3.26972$	$29.48510 + i0.92307$	$31.65836 - i0.89713$
	$10M_W$	$29.10829 + i3.26972$	$29.48510 + i0.92307$	$31.65836 - i0.89713$
ZFITTER		$29.10832 + i3.26973$	$29.48512 + i0.92312$	$31.65835 - i0.89711$
F_{QQ}	$M_W/10$	$44.88226 + i8.85688$	$43.31855 + i9.48287$	$44.18773 + i10.25200$
	M_W	$44.88226 + i8.85688$	$43.31855 + i9.48287$	$44.18773 + i10.25200$
	$10M_W$	$44.88226 + i8.85688$	$43.31855 + i9.48287$	$44.18773 + i10.25200$
ZFITTER		$44.88228 + i8.85688$	$43.31854 + i9.48286$	$44.18773 + i10.25196$

In Table 2 we show a similar comparison with ZFITTER when ZZ boxes are added. As seen, the agreement has not deteriorated.

6.3 eeffLib–ZFITTER comparison of IBA cross-section

As the next step of the comparison of eeffLib with calculations from the literature, we present a comparison of the IBA cross-section.

In Table 3 we show the differential cross-section Eq. (4.44) in pb for three values of $\cos\vartheta = -0.9,\ 0,\ +0.9$, with input parameters of Eq. (6.2) and with constant e.m. coupling $\alpha = \alpha(0)$.

Next, we present the same comparison as in Table 3, but now with running e.m. coupling. Since the flags setting VPOL=1, which is relevant to this case, affects ZFITTER numbers, we now use, instead of Eq. (6.2), the new INPUT set:

$$\begin{aligned} M_W &= 80.4467671 \text{ GeV}, \\ \Delta r &= 0.0284495385\,, \\ \Gamma_Z &= 2.499538 \text{ GeV}. \end{aligned} \tag{6.3}$$

The numbers, shown in first two rows of Tabs. 3 and 4 exhibit a very good level of agreement for light quark masses, while the third rows illustrate the mass effect due to heavy top.

Finally, in Table 5, we give a comparison of the cross-section integrated within the angular interval $|\cos\vartheta| \le 0.999$. (Flags setting is the same as for Table 4.)

Table 3: IBA, First row – ZFITTER ($u\bar{u}$ channel); second row – eeffLib ($m_t = 0.1$ GeV, $m_b = 0$ GeV); third row – eeffLib ($m_t = 173.8$ GeV); with constant e.m. coupling $\alpha = \alpha(0)$.

$\sqrt{s}$	100 GeV	200 GeV	300 GeV	400 GeV	700 GeV	1000 GeV
	47.664652	0.291823	0.169510			
$\cos\vartheta = -0.9$	47.661843	0.291827	0.169515	0.103284	0.035319	0.017204
				0.162193	0.044088	0.018927
	59.768387	1.718830	0.695061			
$\cos\vartheta = 0$	59.770299	1.718870	0.695075	0.376871	0.117279	0.055873
				0.264713	0.112918	0.054209
	168.981978	5.954048	2.292260			
$\cos\vartheta = 0.9$	168.991144	5.954182	2.292302	1.222354	0.372912	0.176038
				0.438453	0.293399	0.154785

Table 4: IBA, First row – ZFITTER ($u\bar{u}$ channel); second row – eeffLib ($m_t = 0.1$ GeV, $m_b = 0$ GeV); third row – eeffLib ($m_t = 173.8$ GeV); with running e.m. coupling $\alpha = \alpha(s)$.

$\sqrt{s}$	100 GeV	200 GeV	300 GeV	400 GeV	700 GeV	1000 GeV
	45.404742	0.386966	0.225923			
$\cos\vartheta = -0.9$	45.404598	0.386966	0.225923	0.138065	0.048621	0.024156
				0.194752	0.058013	0.025959
	60.382423	1.882835	0.771939			
$\cos\vartheta = 0$	60.382562	1.882837	0.771939	0.421410	0.133475	0.064245
				0.303683	0.130173	0.062838
	173.467517	6.450000	2.510881			
$\cos\vartheta = 0.9$	173.467543	6.450000	2.510881	1.346620	0.417295	0.198842
				0.492546	0.330401	0.175564

A typical deviation between eeffLib and ZFITTER is of the order $\sim 10^{-6}$, i.e. of the order of the required precision of the numerical integration over $\cos\vartheta$. Examples of numbers obtained with eeffLib, which were shown in this section, demonstrate that ZFITTER numbers are recovered for light m_t.

We conclude this subsection with a comment about technical precision of our calculations. We do not use looptools package [4]. For all PV functions, but one, namely D_0 function, we use our own coding where we can control precision internally and, typically, we can guarantee 11 digits precision. For D_0 function we use, instead, REAL*16 TOPAZ0 coding [11] and the only accessible for us way to control the precision is to compare results with those computed with looptools package. This was done for a typical D_0 functions entering ZZ box contributions. We got an agreement within 14-15 digits between these two versions for all $\sqrt{s} = 400 - 10000$ GeV and $\cos\vartheta = 0.99,\ 0,\ -0.99$.

Table 5: `eeffLib(L)–ZFITTER(Z)` comparison of the total cross-section. Cross-sections are given in pb: the first row – $\sigma^L_{\rm tot}$, i.e. `eeffLib` ($m_t = 0.1$ GeV); the second row – $\sigma^Z_{\rm tot}$, i.e. `ZFITTER` ($u\bar{u}$ channel); the third row shows the absolute deviation $\sigma^L_{\rm tot} - \sigma^Z_{\rm tot}$.

100 GeV		200 GeV		300 GeV	
$\sigma_{\rm tot}$	$\sigma_{\rm FB}$	$\sigma_{\rm tot}$	$\sigma_{\rm FB}$	$\sigma_{\rm tot}$	$\sigma_{\rm FB}$
160.8981	70.98416	5.021810	3.360848	2.031754	1.269556
160.8980	70.98406	5.021808	3.360848	2.031754	1.269556
0.0001	0.00010	0.000002	0.0	0.0	0.0

6.4 Comparison with a code generated by `s2n_f`

Here we present a numerical comparison of the complete scalar form factors Eq. (3.1) extracted from two independently created codes: 'manually written' `eettLib` and a code, 'automatically generated' by `s2n_f` software. We use a special input parameter set here: all lepton masses α and a conversion factor from GeV^{-1} to pb are taken from 2000 of Particle Data Tables while for quark and photon and gauge boson masses we use:

$$\begin{aligned} m_{u,d,c,s,t,b} &= 0.062,\ 0.083,\ 1.50,\ 0.215,\ 173.8,\ 4.70\ \text{GeV}, \\ \lambda &= 1\ \text{GeV},\ M_Z = zm = 91.1867\ \text{GeV},\ M_W = 80.4514958\ \text{GeV}. \end{aligned} \tag{6.4}$$

Table 6: EWFF for the process $e^+e^- \to t\bar{t}$. `eettLib`, first rows; `s2n_f`, second rows.

$\sqrt{s}$		400 GeV	700 GeV	1000 GeV
$\cos\vartheta$	FF			
-0.9	F_{LL}	$68.36399900074 - i1.24743850729$	$79.63957322115 - i20.53758995637$	$80.47816819240 - i26.71016937527$
		$68.36399900068 - i1.24743850728$	$79.63957322113 - i20.53758995637$	$80.47816819239 - i26.71016937527$
	F_{QL}	$75.12465846647 + i34.81991916400$	$76.19283172015 + i28.44336684106$	$75.95332822621 + i27.77201429453$
		$75.12465846641 + i34.81991916400$	$76.19283172013 + i28.44336684106$	$75.95332822620 + i27.77201429453$
	F_{LQ}	$81.01546270426 + i19.81343626967$	$82.67283873006 + i13.79952080171$	$83.26485989744 + i12.23741074712$
		$81.01546270420 + i19.81343626968$	$82.67283873004 + i13.79952080171$	$83.26485989743 + i12.23741074712$
	F_{QQ}	$225.63977621858 + i154.37838168488$	$207.09189805263 + i133.45188150116$	$194.07155316803 + i134.33226297675$
		$225.63977621832 + i154.37838168491$	$207.09189805254 + i133.45188150117$	$194.07155316799 + i134.33226297675$
	F_{LD}	$-0.57522852857 + i0.34010611241$	$-0.33030593699 + i0.14897150833$	$-0.22418674728 - i0.08847119487$
		$-0.57522852857 + i0.34010611241$	$-0.33030593699 + i0.14897150833$	$-0.22418674728 - i0.08847119487$
	F_{QD}	$0.16677424366 - i0.34326069364$	$0.29925308488 - i0.14107543098$	$0.23436559470 - i0.05839137636$
		$0.16677424366 - i0.34326069364$	$0.29925308488 - i0.14107543098$	$0.23436559470 - i0.05839137636$
0.0	F_{LL}	$48.42950001713 + i8.26103890366$	$28.23570422021 + i2.43705570966$	$16.54896558498 + i0.77082434583$
		$48.42950001707 + i8.26103890367$	$28.23570422019 + i2.43705570966$	$16.54896558497 + i0.77082434583$
	F_{QL}	$68.02678564355 + i37.08805801477$	$58.00469565609 + i33.82433896562$	$52.56343218854 + i34.28418004972$
		$68.02678564349 + i37.08805801477$	$58.00469565607 + i33.82433896562$	$52.56343218853 + i34.28418004972$
	F_{LQ}	$73.37133716227 + i22.69397728402$	$62.40775508619 + i20.75544388763$	$56.94788960099 + i20.65389886886$
		$73.37133716220 + i22.69397728403$	$62.40775508616 + i20.75544388764$	$56.94788960098 + i20.65389886886$
	F_{QQ}	$196.60425612149 + i162.74818773960$	$132.63279537966 + i152.68259938740$	$98.94491326876 + i157.45863002555$
		$196.60425612123 + i162.74818773963$	$132.63279537957 + i152.68259938741$	$98.94491326872 + i157.45863002556$
	F_{LD}	$-0.56319765502 + i0.33645326768$	$-0.29067043403 + i0.13992893252$	$-0.18096486789 + i0.08187546112$
		$-0.56319765502 + i0.33645326768$	$-0.29067043403 + i0.13992893252$	$-0.18096486789 + i0.08187546112$
	F_{QD}	$0.15893936555 - i0.37254018572$	$0.26429138671 - i0.15437851127$	$0.18981891199 - i0.06181088399$
		$0.15893936555 - i0.37254018572$	$0.26429138671 - i0.15437851127$	$0.18981891199 - i0.06181088399$
0.9	F_{LL}	$35.17736865724 + i14.84038724783$	$0.21531292996 + i13.66645015866$	$-18.22896674792 + i13.10520552155$
		$35.17736865718 + i14.84038724784$	$0.21531292994 + i13.66645015866$	$-18.22896674793 + i13.10520552155$
	F_{QL}	$61.03099608330 + i39.09196533610$	$40.77942026097 + i37.94118444135$	$30.73687048410 + i39.06896169999$
		$61.03099608324 + i39.09196533611$	$40.77942026095 + i37.94118444136$	$30.73687048409 + i39.06896169999$
	F_{LQ}	$66.08215572935 + i25.04151178684$	$44.50915974057 + i25.51875704261$	$34.09235431695 + i26.17012224125$
		$66.08215572929 + i25.04151178685$	$44.50915974055 + i25.51875704261$	$34.09235431694 + i26.17012224125$
	F_{QQ}	$167.63393504156 + i170.36384103672$	$59.87568281297 + i168.13599380718$	$7.10290370391 + i175.24101109592$
		$167.63393504130 + i170.36384103675$	$59.87568281288 + i168.13599380719$	$7.10290370387 + i175.24101109593$
	F_{LD}	$-0.56772633347 + i0.34299744419$	$-0.32035310873 + i0.14419510235$	$-0.21547870582 + i0.08254457292$
		$-0.56772633347 + i0.34299744419$	$-0.32035310873 + i0.14419510235$	$-0.21547870582 + i0.08254457292$
	F_{QD}	$0.18031346246 - i0.40091423652$	$0.34968026058 - i0.16945266925$	$0.29109057806 - i0.06775284666$
		$0.18031346246 - i0.40091423652$	$0.34968026058 - i0.16945266925$	$0.29109057806 - i0.06775284666$

As seen from the table numbers agree within 11–13 digits, i.e. `REAL*8` computational precision is saturated. Form factors $F_{LD,QD}$ are multiplied by 10^4 to make more digits visible.

Next Table demonstrates `eettLib`–`s2n_f` comparison for the complete one-loop differential cross-sections $d\sigma^{(1)}/d\cos\vartheta$ for the standard input set. As seen, numbers agree within 12–13 digits.

Table 7: $\dfrac{d\sigma^{(1)}}{d\cos\vartheta}$ for the process $e^+e^- \to t\bar{t}$. `eettLib`–`s2n_f` comparison.

$\sqrt{s}$	400.0	700.0	1000.0
$\cos\vartheta$			
-0.900	0.22357662754774	0.06610825350063	0.02926006442715
	0.22357662754769	0.06610825350063	0.02926006442715
0.000	0.34494634728716	0.14342802645636	0.06752160108814
	0.34494634728707	0.14342802645634	0.06752160108813
0.900	0.54806778978208	0.33837133344667	0.16973989931024
	0.54806778978194	0.33837133344664	0.16973989931023

6.5 About a comparison with the other codes

As is well known, the one-loop differential cross-section of $e^+e^- \to t\bar{t}$ may be generated with the aid of the FeynArts system [4]. Previous attempt to compare with FeynArts are described in [3]. In December 2001, we were provided with the numbers computed with the FeynArts system [13] for $d\sigma/d\cos\vartheta$ with and without QED contributions at $\sqrt{s} = 700$ GeV and three values of $\cos\vartheta = 0.9,\ ,0,\ -0.9$. After debugging of our code `eettLib`, as described in the beginning of this section, we eventually reached 11 digits agreement both for the tree level and one-loop corrected cross-sections.

We do not update Fig.13 and Fig.14 of [3], since the differences with updated version is not seen.

Table 8: $\dfrac{d\sigma^{(1)}}{d\cos\vartheta}$ for the process $e^+e^- \to t\bar{t}$ with soft photons, $E_\gamma^{\max} = \sqrt{s}/10$.

$\sqrt{s}$	400.0	700.0	1000.0
$\cos\vartheta$			
-0.900	0.17613018248935	0.05199100267864	0.02310170508071
-0.500	0.21014509428358	0.06560630503586	0.02882301902010
0.000	0.27268108572063	0.11496514450150	0.05495088904853
0.500	0.35592722356682	0.19615154401629	0.09941700898317
0.900	0.43637377538440	0.27915043976042	0.14426233253975

Recently, a Bielefeld–Zeuthen team [5] performed an alternative calculations using the DIANA system [12]. Working in close contact with this team, we managed to perform several high-precision comparisons reaching for separate contributions an agreement in 10 digits.

The results of a comparison between FeynArts and Bielefeld–Zeuthen team are presented in detail in [6].

As another example we present in Table 8 the same cross-section $[d\sigma/d\cos\vartheta]_{\rm SM}$ as given in tables of [6]. For the complete cross-section, including soft photons, we agree with Bielefeld–Zeuthen calculations within 7-8 digits.

Acknowledgements

We would like to thank W. Hollik and C. Schappacher for a discussion of issues of the comparison with FeynArts. We acknowledge a common work on numerical comparison with J. Fleischer, A. Leike, T. Riemann, and A. Werthenbach which helped us to debug our 'manually written' code `eettLib`. We also wish to thank G. Altarelli for extending to us the hospitality of the CERN TH Division at various stages of this work.

[1] M. Beneke *et al.*,'Top quark physics', in *Proc. of the Workshop on Standard Model Physics (and More) at the LHC*, CERN 2000–004 (G. Altarelli and M. Mangano, eds.), pp. 419–529, 2000.

[2] D.Bardin, G.Passarino, L.Kalinovskaya, P.Christova, A.Andonov, S.Bondarenko and G.Nanava, 'Project `CalcPHEP`: Calculus for Precision High Energy Physics', 2002, `hep-ph/0202004`.

[3] D.Yu. Bardin, L.V. Kalinovskaya, G. Nanava, 'An electroweak library for the calculation of EWRC to $e^+e^- \to f\bar{f}$ within the `CalcPHEP` project.' JINR-E2-2000-292, Dec 2000. e-Print Archive: hep-ph/0012080, Revised version, CERN-TH/2001-308, November 2001.

[4] J. Küblbeck, M. Böhm, A. Denner, *Comput. Phys. Commun.* **60** (1990) 165; T. Hahn, M. Perez-Victoria, *Comput. Phys. Commun.* **118** (1999) 153; T. Hahn, *Nucl. Phys. Proc. Suppl.* **89** (2000) 231; T. Hahn, *Comput. Phys. Commun.* **140** (2001) 418; T. Hahn, C. Schappacher, `hep-ph/0105349`.

[5] J. Fleischer, T. Riemann, and A. Werthenbach, private communication.

[6] J. Fleischer, T. Hann, W. Hollik, T. Riemann, C. Schappacher, and A. Werthenbach, 'Complete electroweak one-loop radiative corrections to top-pair production at **TESLA** - a comparison - ', LC-TH-2002-002, `hep-ph/0202109`.

[7] R. Vega and J. Wudka, A Covariant Method for Calculating Helicity Amplitudes, (SMU-HEP-94/28) `hep-ph/9511318v1` (1995).

[8] D. Bardin and G. Passarino, 'The standard model in the making: Precision study of the electroweak interactions', Oxford, UK: Clarendon, 1999.

[9] D. Bardin, M. Bilenky, P. Christova, M. Jack, L. Kalinovskaya, A. Olchevski, S. Riemann, and T. Riemann, ZFITTER v.6.30, obtainable from `http://www.ifh.de/~riemann/` and from `/afs/cern.ch/user/b/bardindy/public`.

[10] D. Bardin, M. Bilenky, P. Christova, M. Jack, L. Kalinovskaya, A. Olchevski, S. Riemann, and T. Riemann, 'ZFITTER v.6.21: A semi-analytical program for fermion pair production in e^+e^- annihilation', DESY–Zeuthen preprint 99-070 (1999), `hep-ph/9908433`, *Comput. Phys. Commun.*, **133** (2001) 229–395.

[11] G. Montagna, O. Nicrosini, F. Piccinini and G. Passarino, *Comput. Phys. Commun.* **117** (1999) 278.

[12] J. Fleischer and M. Tentyukov, 'A Feynman Diagram Analyser DIANA' - Graphic Facilities, Contribution to the Proceedings of 7th International Workshop on Advanced Computing and Analysis Techniques in Physics Research (ACAT 2000), Batavia, Illinois, 2000, `hep-ph/0012189`.

[13] The numbers for the comparison were provided by C. Schappacher.